Modeling peristaltic flow in vessels equipped with valves: implications for vasomotion in bat wing venules

A. Farina[1], L. Fusi[1], A. Fasano[2,3,4], A. Ceretani[5], F. Rosso[1]

[1]Università degli Studi di Firenze
Dipartimento di Matematica "U. Dini"
Università degli studi di Firenze, Firenze, Italy

[2]Professor Emeritus, Università degli Studi di Firenze
Dipartimento di Matematica e Informatica "U. Dini", Firenze, Italy

[3]Scientific Manager FIAB SpA, Firenze, Italy

[4]Associated to IASI-CNR, Roma, Italy

[5]CONICET - Facultad de Ciencias Empresariales, Universidad Austral
Depto. Matematica, Paraguay 1950, S2000FZF
Rosario, Argentina

Abstract

The phenomenon of vasomotion, consisting in periodic oscillations of blood vessels walls is particularly important for the flow venules provided with valves preventing back flow. Here we formulate a mathematical model for based on approximations of the flow equations implied by the smallness of the radius-to-length ratio. For venules we postulate the presence of just two valves and we show that the model reproduces the periodic pressure pulses that have been detected in the experimental literature devoted to venules of the bat wing. In addition, the flow generated by the syncronous vessel oscillation is recovered as the limit of the flow generated by the vessel peristalsis in the limit of large wavelength.

1 Introduction

Blood vessels equipped with smooth muscle cells may undergo radial oscillations that are independent on heart pulsation or respiratory rhythm, and have indeed a different frequency. This phenomenon, called vasomotion, was first observed by T.W. Jones [17] in 1852 in the venules of the bat wing. Its biological mechanisms have been studied in a number of papers. See the reviews [22], [13], [1] and the papers [21], [29], [20], [3], [14], [23], and [19] proposing various mathematical models for the onset of persisting oscillations. Vasomotion frequency can (exceptionally) reach 25 cpm and amplitude can peak to 100% of mean diameter [15]. More ordinary values are 10 cpm and 25%. Since vasomotion is particularly active right where vessels resistance becomes large, it is a phenomenon considered with great attention, since it may have a critical influence on microcirculation.

In the recent paper [4] the authors, experimenting with bat wings, proved that venules vasomotion acts as a pump, increasing blood flow rate, thanks to the presence of backflow preventing valves. The experiments of [4] show that pressure exhibits large peaks during the vessel contraction, which is compatible with the presence of an inlet and an outlet valves.

In this paper we formulate a mathematical model for an incompressible Newtonian flows in a cylindrical tubes, representing the venule. The tube walls, contracting and expanding periodically, act as a peristaltic pump. The tube has two valves: one at the entrance and the other at the outlet. Though we exploit the

smallness of the ratio[1]

$$\varepsilon = \frac{R_o^*}{L^*} \ll 1. \tag{1.1}$$

where R_o^* is the maximum vessel radius and L^* is the vessel length, the interaction flow-vasomotion is quite complicated because of the action of valves. Following [4], we consider each valve as a compliant membrane which opens (respectively closes) when the pressure on its left side is larger (respectively smaller) than the one on its right side. The valve's action is thus modeled imposing a unilateral, or Signorini, boundary condition, which, in the authors' knowledge, is a novelty.

The analysis of the peristaltic flow, in a low Reynolds number and lubrication theory context, has been developed in a number of papers. Here we just mention [10], [24], [2], [31], devoted to the peristaltic wave optimal shape, and [27] in which the coupling between the flow and mechanics of the tube wall is studied. On the other hand, the literature treating peristaltic flow in vessels equipped with valves is not very vast. We mention the pioneering paper [28] in which the flow in semi-infinite cylindrical vessel is analyzed. The paper focuses on the laminar flow driven by the wall contraction-expansion, but does not consider the open-close mechanism of the inlet valve (the longitudinal velocity is set zero at the inlet valve). Also the peristaltic flow in micro-devices equipped with valves has recently received attention in the context of the micro pumping technologies. In such a framework, the valves are devices of various nature whose purpose is to make unidirectional the flow. We mention the interesting review [16] and [12] where a model for peristaltic micro-pumps with active valves has been developed. However the fluid mechanical setting considered in [12], as well as in many other papers devoted to micro pumping technologies, is totally different form the one we are considering in this paper. Moreover, the models developed in those papers do not consider the dynamic of the flow, being essentially oriented toward the overall functioning of the device.

The model we develop in this paper considers an incompressible Newtonian fluid and a contraction-expansion wave travelling along the vessel. In particular, denoting by λ^* the oscillation wavelength, we investigate two cases:

- $\lambda^* \gg L^*$, referred to as synchronous oscillation.
- $\lambda^* \approx L^*$, referred to as non synchronous oscillation.

The first case consists essentially in a uniform oscillation of the vessel walls, and, thanks to the inlet outlet valves, we have a net flow. Indeed, if the vessel had no valves, the wall oscillations would produce, on average, zero flow. The action of the inlet and outlet membranes converts the non-directional flow to directional flow.

In the second case a wave profile travels along the vessel. Now, contrary to the first case, we can have, also in valveless tube, a non-zero average flow even if the external pressure gradient vanishes. However, inlet and outlet backflows occur in valveless tubes, while in vessels equipped with valves the inlet and outlet flows stay unidirectional.

The paper develops as follows: in § 2 we present the mathematical model. In particular, § 2.3 is devoted to a detailed discussion of the inlet and outlet boundary conditions. The synchronous oscillation model is illustrated in § 3, while the non synchronous oscillation in § 4. In § 5 we present some numerical simulations which, highlight physical consistency of the model. We indeed show that the first case (synchronous oscillation) is recovered from the second one in the limit of "long" wavelengths. Last but not least, in § 6 we show numerical solutions that are close to the experimentally detected pressure behavior displayed in [4].

2 Flow in a vessel equipped with an inlet and outlet valve

The physical effect of vasomotion on blood flow in venules equipped with valves preventing backflow is completely different from the one occurring in a valveless vessels. Indeed the valves confer to vasomotion a pumping action, whose contribution to the flow may be comparable to the one of the available pressure gradient.

While valves in the major veins had been observed since the early times of anatomy[2], the presence of valves in small veins has been underestimated or even ignored. The paper [5] reviews the historical perspective on

[1] The symbol " * " denotes dimensional quantities.

[2] There is some controversy about the discovery of vein valves. According to A. Caggiati the first to describe them was the Catalan Ludovicus Vassaeus in his *De Anatomen Corporis Humani tabulae quator* (Venice, 1542). See [6], [7], [5]. There were more or less contemporary or even earlier observations. In the old review paper [9] reference is made to unpublished findings on the subject by Giambattista Canano (1515-1579), professor of anatomy in Ferrara, that he reported to Vesalius in 1545. In the same

the subject, particularly concerning microscopic valves, whose existence has been proved in venules as small as 25 μm diameter, where they may be arranged in series (see [6], [7]).

With the target of fitting some of the experimental data of [4], we formulate a novel model for vessel equipped with just two valves placed at $x^* = 0$ and $x^* = L^*$, corresponding to vessel's inlet and outlet. The behavior of pressure shown in [4] cannot be explained without the presence of valves that act synchronously with the vessel oscillation. Indeed, a model with distributed valves, as the one developed in [8], cannot explain the pressure peaks detected in [4], since such a model encompasses a condition of pressure continuity which forces pressure to stay between the imposed inlet and outlet values.

2.1 The mathematical model

Let us now suppose that the vessel radius R^* evolves as a travelling wave with wavelength λ^*, i.e.

$$R^*(x^*, t^*) = R_o^* R(x^*, t^*), \qquad R(x^*, t^*) = 1 + \delta\Phi\left(\frac{x^*}{\lambda^*} - \frac{t^*}{T^*}\right), \tag{2.1}$$

where:

- $\Phi(\eta)$ is a periodic function (with period 1) such that $\max\Phi = 0$, $\min\Phi = -1$. We suppose also that Φ is decreasing in a fraction of the period (contraction phase) and increasing in the remaining fraction (expansion phase). In the physiological case of vasomotion the contraction fraction is typically < 0.5, [4].
- R_o^* is the maximum radius.
- $0 < \delta < 1$, is a dimensionless parameter, so that $R_o^*\delta$, gives the oscillation amplitude.
- λ^* is the wavelength and T^* is the wave period, which are linked to the wave velocity c^* by

$$c^* = \frac{\lambda^*}{T^*}. \tag{2.2}$$

We denote by $\boldsymbol{u}^*$ the tube surface velocity directed along the radius. From (2.1)

$$\boldsymbol{u}^* = \frac{\partial R^*}{\partial t^*}\boldsymbol{e}_r = -\dot{R}_{ref}^*\Phi'\left(\frac{x^*}{\lambda^*} - \frac{t^*}{T^*}\right)\boldsymbol{e}_r, \tag{2.3}$$

where $\Phi'(\eta) = d\Phi/d\eta$ and where

$$\dot{R}_{ref}^* = \frac{R_o^*\delta}{T^*}, \tag{2.4}$$

represents the average contraction velocity, so that we set $v_{2\ ref} = \dot{R}_{ref}^*$. In vasomotion $\dot{R}_{ref}^*$ is available from experiments. We introduce also $\lambda = \lambda^*/L^*$. As already stated in the introduction, we consider two cases:

1. λ^* much larger than L^* (more precisely $\lambda^{-1} \leq \varepsilon$), meaning that the vessel essentially undergoes spatially synchronous oscillations.
2. λ^* comparable with L^* i.e. $\lambda = \mathcal{O}(1)$.

In [11] we proved that when $\lambda^* \ll L^*$, peristalsis basically does not generate any flow. In dimensionless variables (2.1) becomes

$$R(x, t) = 1 + \delta\Phi\left(\frac{x}{\lambda} - t\right), \tag{2.5}$$

so that

$$\lambda\frac{\partial R}{\partial x} + \frac{\partial R}{\partial t} = 0.$$

The fluid enters the tube through the inlet surface $\{x^* = 0,\ 0 \leq r^* \leq R^*(0, t^*)\}$ and flows out through the outlet surface $\{x^* = L^*,\ 0 \leq r^* \leq R^*(L^*, t^*)\}$.

year veins valves were described by the French anatomist Charles Estienne (1504-1564), who however claimed to have discovered them in 1538.

We select the longitudinal reference velocity v^*_{ref} as follows

$$v^*_{ref} = \frac{1}{\varepsilon}\dot{R}^*_{ref} = \frac{1}{\varepsilon}\frac{R^*_o \delta}{T^*}. \tag{2.6}$$

So, if $\boldsymbol{v}^* = v^*_1\ \boldsymbol{e}_x + v^*_2\ \boldsymbol{e}_r$ is the fluid velocity, we set

$$v_1 = \frac{v^*_1}{v^*_{ref}}, \qquad v_2 = \frac{v^*_2}{\dot{R}^*_{ref}} = \frac{v^*_2}{\varepsilon v^*_{ref}},$$

entailing $\boldsymbol{v} = \ v_1\boldsymbol{e}_x + \varepsilon v_2\ \boldsymbol{e}_r$. The reference pressure p^*_{ref} is defined as

$$\frac{p^*_{ref}}{L^*} = \frac{\mu^*}{{R^*_o}^2} v^*_{ref}\ .$$

The quantity p^*_{ref} represents the order of magnitude of the "effective pressure drop" caused by the oscillations of the vessel (inspired to Poiseuille's formula). The known imposed pressure difference is $\Delta p^* = p^*(0,t^*) - p^*(L^*,t^*)$, and we consider

$$\Delta p = \frac{\Delta p^*}{p^*_{ref}} \leq \mathcal{O}(1).$$

When $\Delta p \gg 1$, the flow is essentially dominated by the externally imposed pressure gradient and the effects due to the wall oscillations are hardly observable. We also introduce the dimensionless pressure

$$p = \frac{p^*(x^*,t^*) - p^*(L^*,t^*)}{p^*_{ref}}, \tag{2.7}$$

so that

$$p|_{inlet} = \Delta p, \qquad p|_{outlet} = 0. \tag{2.8}$$

We finally rescale the radial velocity of the vessel walls $\boldsymbol{u}^*$ by $\dot{R}^*_{ref}$, namely

$$\boldsymbol{u}^* = \dot{R}^*_{ref}\ u\ \boldsymbol{e}_r, \quad \text{with} \quad u = -\Phi'\left(\frac{x}{\lambda} - t\right) = -\frac{\lambda}{\delta}\frac{\partial R}{\partial x} = \frac{1}{\delta}\frac{\partial R}{\partial t}. \tag{2.9}$$

2.2 Flow equations

The fluid mechanical incompressibility yields

$$\frac{\partial v_1}{\partial x} + \frac{1}{r}\frac{\partial (r v_2)}{\partial r} = 0. \tag{2.10}$$

We assume that the Reynolds number characterizing the flow

$$\mathsf{Re} = \frac{\rho^* v^*_{ref} R^*_o}{\mu^*}\ ,$$

is negligible[3] so that the motion equation reduces to

$$-\nabla^* p^* + \mu^* \Delta^* \boldsymbol{v}^* = 0. \tag{2.11}$$

On the tube surface we set $\boldsymbol{v}^*|_{r^*=R^*} = \boldsymbol{u}^*$ so that, from (2.3)

$$v_1|_{r=R} = 0, \tag{2.12}$$

$$v_2|_{r=R} = u \underset{(2.9)}{=} -\Phi'\left(\frac{x}{\lambda} - t\right) = \frac{\partial \Phi}{\partial t} = -\frac{1}{\lambda}\frac{\partial \Phi}{\partial x}. \tag{2.13}$$

[3]Referring, for instance, to the data of [4] we have $\mathsf{Re} \approx 10^{-2}$.

The line $r = 0$ is a symmetry axis so that

$$v_2|_{r=0} = 0, \quad \text{and} \quad \left.\frac{\partial v_1}{\partial r}\right|_{r=0} = 0. \tag{2.14}$$

Equations (2.11) become

$$-\frac{\partial p}{\partial x} + \varepsilon^2 \frac{\partial^2 v_1}{\partial x^2} + \frac{1}{r}\frac{\partial}{\partial r}\left(r\frac{\partial v_1}{\partial r}\right) = 0, \tag{2.15}$$

$$-\frac{1}{\varepsilon^2}\frac{\partial p}{\partial r} + \varepsilon^2 \frac{\partial^2 v_2}{\partial x^2} + \frac{1}{r}\frac{\partial}{\partial r}\left(r\frac{\partial v_2}{\partial r}\right) - \frac{v_2}{r^2} = 0, \tag{2.16}$$

which, at the leading order imply

$$p = p\left(x,t\right),$$

and

$$-\frac{\partial p}{\partial x} + \frac{1}{r}\frac{\partial}{\partial r}\left(r\frac{\partial v_1}{\partial r}\right) = 0. \tag{2.17}$$

Recalling boundary conditions (2.12) and $(2.14)_2$, we find

$$v_1\left(x,r,t\right) = -\frac{1}{4}\frac{\partial p}{\partial x}\left(R^2 - r^2\right), \tag{2.18}$$

with $R\left(x,t\right)$ given by (2.5). We now insert (2.18) in (2.10), getting

$$4\frac{\partial}{\partial r}\left(r\, v_2\right) = \frac{\partial^2 p}{\partial x^2} r\left(R^2 - r^2\right) + 2r\frac{\partial p}{\partial x}R\frac{\partial R}{\partial x}.$$

Integrating between 0 and R and exploiting (2.13) we obtain

$$\frac{\partial}{\partial x}\left(\frac{R^4}{4}\frac{\partial p}{\partial x}\right) = 4Ru, \tag{2.19}$$

with u given by (2.9). So, taking the average on the vessel section, we have

$$\langle v_1\rangle = \frac{2}{R^2}\int_0^R \left(-\frac{1}{4}\frac{\partial p}{\partial x}\right)\left(R^2 - r^2\right) r dr = -\frac{1}{8}\frac{\partial p}{\partial x}R^2,$$

while the local discharge at time t (within an $\mathcal{O}\left(\varepsilon\right)$ approximation)

$$Q\left(x,t\right) = \pi R^2 \langle v_1\rangle = -\pi\frac{R^4}{8}\frac{\partial p}{\partial x}. \tag{2.20}$$

2.3 Boundary conditions at the vessel ends

The valves are placed at the vessels ends, and act to prevent backflow. The valves dynamics is indeed simple: the inlet valve closes when pressure exceeds the inlet one; the outlet valve closes when pressure falls below the outlet one. In other words, at $x = 0$, inlet valve, two conditions have to be fulfilled

$$Q\left(0,t\right) \geq 0, \quad \Leftrightarrow \quad \left.\frac{\partial p}{\partial x}\right|_{x=0} \leq 0, \tag{2.21}$$

$$p\left(0,t\right) \geq \Delta p. \tag{2.22}$$

The first condition simply states that backflow cannot occur, while the second one guarantees that $p\left(0,t\right)$ can never drop below the imposed pressure. Moreover, it is necessary that at least one of such condition holds as an equality. Hence the inlet boundary conditions summarize as follows

$$\begin{cases} \left.\dfrac{\partial p}{\partial x}\right|_{x=0}\left(p\left(0,t\right) - \Delta p\right) = 0 \\ \\ \left.\dfrac{\partial p}{\partial x}\right|_{x=0} \leq 0, \\ \\ p\left(0,t\right) \geq \Delta p. \end{cases} \tag{2.23}$$

This is a typical unilateral boundary condition - also known as Signorini type condition - which is frequently encountered in continuum mechanics (see, for instance, [18]). Similarly, the boundary conditions at $x = 1$ are

$$\begin{cases} \left.\dfrac{\partial p}{\partial x}\right|_{x=1} p\left(1,t\right) = 0, \\ \\ \left.\dfrac{\partial p}{\partial x}\right|_{x=1} \leq 0, \\ \\ p\left(1,t\right) \leq 0. \end{cases} \tag{2.24}$$

3 First case: $\lambda^{-1} \leq \varepsilon$: synchronous oscillation

This case, as stated more than once, corresponds to a spatially uniform contraction/expansion of the vessel. Therefore $R = R\left(t\right)$ and, because of (2.9),

$$u = \frac{1}{\delta}\dot{R}\left(t\right).$$

Formula (2.19) can be rewritten as

$$\frac{\partial^2 p}{\partial x^2} = \frac{16}{\delta}\frac{\dot{R}}{R^3}, \quad \Rightarrow \quad \begin{cases} p\left(x,t\right) = \dfrac{8}{\delta}\dfrac{\dot{R}\left(t\right)}{R^3\left(t\right)}x^2 + A\left(t\right)x + B\left(t\right), \\ \\ \dfrac{\partial p\left(x,t\right)}{\partial x} = \dfrac{16}{\delta}\dfrac{\dot{R}\left(t\right)}{R^3\left(t\right)}x + A\left(t\right), \end{cases}$$

where $A\left(t\right)$, $B\left(t\right)$ have to be determined. Interestingly

$$\frac{\dot{R}}{R^3} = -\frac{\pi}{2}\frac{d}{dt}\left(\frac{1}{S\left(t\right)}\right),$$

where $S\left(t\right) = \pi R^2\left(t\right)$ is the vessel section. Condition (2.23) rewrites as

$$\begin{cases} A\left(t\right)\left(B\left(t\right) - \Delta p\right) = 0, \\ \\ A\left(t\right) \leq 0, \\ \\ B\left(t\right) - \Delta p \geq 0, \end{cases} \tag{3.1}$$

while (2.24) takes the form

$$\begin{cases} \left(\dfrac{8}{\delta}\dfrac{\dot{R}\left(t\right)}{R^3\left(t\right)} + A\left(t\right) + B\left(t\right)\right)\left(\dfrac{16}{\delta}\dfrac{\dot{R}\left(t\right)}{R^3\left(t\right)} + A\left(t\right)\right) = 0, \\ \\ \dfrac{16}{\delta}\dfrac{\dot{R}\left(t\right)}{R^3\left(t\right)} + A\left(t\right) \leq 0, \\ \\ \dfrac{8}{\delta}\dfrac{\dot{R}\left(t\right)}{R^3\left(t\right)} + A\left(t\right) + B\left(t\right) \leq 0. \end{cases} \tag{3.2}$$

Let us consider the compression phase $\dot{R} < 0$, and assume first $A = 0$ (entrance valve engaged). From $(3.2)_1$

$$B\left(t\right) = \frac{8}{\delta}\frac{\left|\dot{R}\right|}{R^3},$$

meaning $p(1,t)=0$. Of course condition $(3.1)_3$ has to be satisfied so that

$$\frac{8}{\delta}\frac{\left|\dot{R}\right|}{R^3} \geq \Delta p. \tag{3.3}$$

On the other hand if

$$\frac{8}{\delta}\frac{\left|\dot{R}\right|}{R^3} < \Delta p, \tag{3.4}$$

the entrance valve is open and the solution is

$$B(t)=\Delta p \quad \text{and} \quad A(t)=-\left(\frac{8}{\delta}\frac{\dot{R}(t)}{R^3(t)}+\Delta p\right).$$

Hence, during the compression phase we have

$$p(x,t)=\begin{cases} \dfrac{8}{\delta}\dfrac{\dot{R}}{R^3}\left(x^2-1\right), & \text{if} \quad \dfrac{8}{\delta}\dfrac{\left|\dot{R}\right|}{R^3} \geq \Delta p, \\ \dfrac{8}{\delta}\dfrac{\dot{R}}{R^3}\left(x^2-x\right)-\Delta p\,(x-1), & \text{if} \quad \dfrac{8}{\delta}\dfrac{\left|\dot{R}\right|}{R^3} < \Delta p, \end{cases} \tag{3.5}$$

corresponding to a closed or open entrance valve. In the expansion phase $\dot{R}>0$, we first consider

$$A=-\frac{16}{\delta}\frac{\dot{R}}{R^3},$$

i.e. the exit valve is closed. We conclude that B equals the inlet dimensionless pressure $B(t)=\Delta p$ and, recalling $(3.2)_3$, we observe that the compatibility condition (3.3) must once again be fulfilled. On the other hand, when condition (3.4) holds the exit valve is open and the condition $p(1,t)=0$ yields

$$A(t)=-\left(\frac{8}{\delta}\frac{\dot{R}(t)}{R^3(t)}+\Delta p\right) \quad \text{and} \quad B(t)=\Delta p.$$

Summarizing, during the expansion phase the pressure is

$$p(x,t)=\begin{cases} \Delta p+\dfrac{8}{\delta}\dfrac{\dot{R}}{R^3}\left(x^2-2x\right), & \text{if} \quad \dfrac{8}{\delta}\dfrac{\dot{R}}{R^3} \geq \Delta p, \\ \dfrac{8}{\delta}\dfrac{\dot{R}}{R^3}\left(x^2-x\right)-\Delta p\,(x-1), & \text{if} \quad \dfrac{8}{\delta}\dfrac{\dot{R}}{R^3} < \Delta p, \end{cases} \tag{3.6}$$

corresponding to a closed or open exit valve. We remark that when $\dot{R}=0$ equations (3.5)-(3.6) provides the classical linear profile

$$p(x,t)=\Delta p\ (1-x).$$

We also observe that when a valve at one end is closed the one at the opposite end is open, so that the flux has no interruption.

4 Second case: $\lambda = \mathcal{O}(1)$: non-synchronous oscillation

Recalling (2.19) and (2.9), we write

$$\frac{\partial}{\partial x}\left(\frac{R^4}{8}\frac{\partial p}{\partial x}\right) = -\frac{\lambda}{\delta}\frac{\partial R^2}{\partial x}. \tag{4.1}$$

Integrating once we get

$$\frac{\partial p}{\partial x} = -\frac{8\lambda}{\delta}\frac{1}{R^2} + \frac{\mathcal{A}(t)}{R^4}, \tag{4.2}$$

where $\mathcal{A}(t)$ is unknown at this stage. Integrating once more

$$p(x,t) \ = \mathcal{B}(t) - \frac{8\lambda}{\delta}\int_0^x \frac{dx'}{R^2} + \mathcal{A}(t)\int_0^x \frac{dx'}{R^4},$$

where $\mathcal{B}(t)$ is unknown as well.

Remark 1 *Exploiting (2.20), formula (4.1) can be rewritten as*

$$\frac{\partial Q(x,t)}{\partial x} = \frac{\pi\lambda}{\delta}\frac{\partial R^2}{\partial x}, \quad \Rightarrow \quad Q(x,t) = \frac{\pi\lambda}{\delta}R^2(x,t) + F(t).$$

The latter allows to evaluate the mean difference between the inlet discharge (i.e. at $x = 0$) and the outlet discharge (at $x = 1$), namely

$$\langle \Delta Q(t) \rangle = \int_0^1 [Q(0,t) - Q(1,t)]dt.$$

We have

$$\langle \Delta Q(t) \rangle = \frac{\pi\lambda}{\delta}\left(\int_0^1 R^2(0,t)dt - \int_0^1 R^2(1,t)dt\right) = 0,$$

showing that the inlet and outlet mean discharges are equal

We introduce

$$R_{in}(t) = R(0,t), \quad R_{out}(t) = R(1,t), \quad S_{in}(t) = \pi R_{in}^2(t), \quad S_{out}(t) = \pi R_{out}^2(t),$$

and, proceeding as in § 3, we consider two cases:

$$(a) \qquad S_{in}(t) < S_{out}(t) \quad \Leftrightarrow \quad R_{in}(t) < R_{out}(t)$$

$$(b) \qquad S_{in}(t) \geq S_{out}(t) \quad \Leftrightarrow \quad R_{in}(t) \geq R_{out}(t)$$

We define

$$\mathcal{I}_2(t) = \int_0^1 \frac{dx}{R^2(x,t)}, \qquad \mathcal{I}_4(t) = \int_0^1 \frac{dx}{R^4(x,t)}.$$

In case (a) the boundary conditions (2.23), (2.24) yields

$$\mathcal{A}(t) = \frac{8\lambda}{\delta}R_{in}^2(t),$$

and

$$\mathcal{B}(t) = \frac{8\lambda}{\delta}\left[\mathcal{I}_2(t) - R_{in}^2(t)\,\mathcal{I}_4(t)\right],$$

provided

$$\frac{8\lambda}{\delta}\left[\mathcal{I}_2(t) - R_{in}^2(t)\,\mathcal{I}_4(t)\right] \geq \Delta p\,.$$

On the other hand, when

$$\Delta p > \frac{8\lambda}{\delta}\left[\mathcal{I}_2(t) - R_{in}^2(t)\,\mathcal{I}_4(t)\right], \tag{4.3}$$

we take

$$\mathcal{B}(t) = \Delta p,$$

and

$$\mathcal{A}(t) = \frac{\frac{8\lambda}{\delta}\mathcal{I}_2(t) - \Delta p}{\mathcal{I}_4(t)}, \tag{4.4}$$

Since conditions $(2.23)_3$ and $(2.24)_3$ are fulfilled, we need to prove only $(2.23)_2$ from which $(2.24)_2$ automatically follows because $R_{in}^2 < R_{out}^2$. Rewriting $(2.23)_2$ as

$$\mathcal{A} \leq \frac{8\lambda}{\delta} R_{in}^2$$

and using (4.4), we immediately obtain (4.3). Concerning case (b), we have

$$\mathcal{B} = \Delta p,$$

and

$$\mathcal{A}(t) = \frac{8\lambda}{\delta} R_{out}^2(t), \quad \text{if} \quad \Delta p \leq \frac{8\lambda}{\delta}\left[\mathcal{I}_2(t) - R_{out}^2(t)\,\mathcal{I}_4(t)\right],$$

or $\mathcal{A}$ given by (4.4) in case $\Delta p > \frac{8\lambda}{\delta}\left[\mathcal{I}_2(t) - R_{out}^2(t)\,\mathcal{I}_4(t)\right]$. We have thus proved the following

- If $S_{in} < S_{out}$, and $\Delta p \leq \frac{8\lambda}{\delta}\left[\mathcal{I}_2(t) - R_{in}^2(t)\,\mathcal{I}_4(t)\right]$ then

$$p(x,t) = \frac{8\lambda}{\delta}\int_x^1 \left(\frac{1}{R^2(x',t)} - \frac{R_{in}^2(t)}{R^4(x',t)}\right) dx'. \tag{4.5}$$

- If $S_{in} < S_{out}$, and $\Delta p > \frac{8\lambda}{\delta}\left[\mathcal{I}_2(t) - R_{in}^2(t)\,\mathcal{I}_4(t)\right]$ then

$$p(x,t) = \Delta p\left(1 - \frac{1}{\mathcal{I}_4(t)}\int_0^x \frac{dx'}{R^4}\right) + \frac{8\lambda}{\delta}\int_0^x \left(\frac{1}{R^4}\frac{\mathcal{I}_2(t)}{\mathcal{I}_4(t)} - \frac{1}{R^2}\right) dx'. \tag{4.6}$$

- If $S_{in} \geq S_{out}$, and $\Delta p \leq \frac{8\lambda}{\delta}\left[\mathcal{I}_2(t) - R_{out}^2(t)\,\mathcal{I}_4(t)\right]$ then

$$p(x,t) = \Delta p + \frac{8\lambda}{\delta}\int_0^x \left(\frac{R_{out}^2}{R^4} - \frac{1}{R^2}\right) dx'. \tag{4.7}$$

- If $S_{in} \geq S_{out}$, and $\Delta p > \frac{8\lambda}{\delta}\left[\mathcal{I}_2(t) - R_{out}^2(t)\,\mathcal{I}_4(t)\right]$ then

$$p(x,t) = \Delta p\left(1 - \frac{1}{\mathcal{I}_4(t)}\int_0^x \frac{dx'}{R^4}\right) + \frac{8\lambda}{\delta}\int_0^x \left(\frac{1}{R^4}\frac{\mathcal{I}_2(t)}{\mathcal{I}_4(t)} - \frac{1}{R^2}\right) dx'. \tag{4.8}$$

5 Numerical simulations: synchronous and non synchronous oscillations

In this section we provide some numerical simulations to show the qualitative behavior of the solution. We begin by showing the behavior of the pressure selecting the function $\Phi(\eta)$ defined in (2.1) in the following way

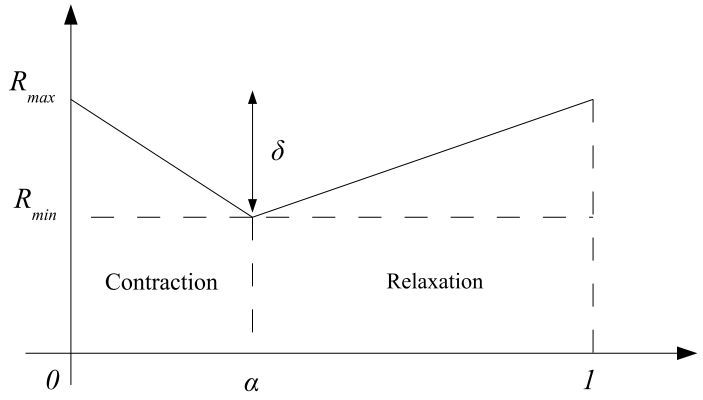

Figure 1: The function $R(\eta)$.

$$\Phi(\eta) = \begin{cases} -\dfrac{\eta}{\alpha}, & \eta \in [0, \alpha], \\ \\ -1 + \dfrac{(\eta - \alpha)}{(1 - \alpha)}, & \eta \in [\alpha, 1]. \end{cases}$$

This selection implies that the oscillation is formed by a contraction ($\alpha-$fraction of the period) and an expansion ($(1-\alpha)-$fraction of the period). The function $R(\eta)$ (Fig. 1) is thus

$$R(\eta) = \begin{cases} 1 - \dfrac{\delta\eta}{\alpha}, & \eta \in [0, \alpha], \\ \\ (1 - \delta) + \dfrac{\delta(\eta - \alpha)}{(1 - \alpha)}, & \eta \in [\alpha, 1]. \end{cases} \tag{5.1}$$

The choice of R is purely illustrative: other choices are clearly possible. In Fig.s 2, 3 we plot the pressure profile $p(x,t)$ for different values of λ using the expressions (4.5)-(4.8) derived in § 4. In particular, we plot p as a function of x for $t \in [0,1]$. The inlet pressure Δp is taken equal to one. As one can see, when λ approaches $O(10^3)$, the pressure plots stabilize, so that a further increase of λ does not produce any change in the pressure profiles. This fact can be explained observing that for λ sufficiently large the oscillation is essentially synchronous (i.e. spatially uniform).

We remark that the model is physically consistent, since the plot corresponding to the synchronous oscillation essentially coincides with the plot corresponding to the non synchronous oscillation with $\lambda \gg 1$ (see Fig. 4).

6 Comparison with experimental data

In order to compare our model with the experimental data provided in [4] we consider a synchronous (dimensional) oscillation $R^*(t^*)$ that reproduces the experimental recording of the diameter change of a representative venule, as shown in Fig. 3 of [4]. In particular we select a non dimensional $R(t)$ of the type[4]

$$R(t) = at^3(1 - t^3)^3 + (1 - \delta). \tag{6.1}$$

and we use the parameter a to fit the experimental R^*. From Fig. 3 of [4] we notice that $R^*_o \approx 70 : \mu m$, $T^* \approx 6 : sec$, $\delta = 0.25$, so that we can easily find the fitting parameter a, which turns out to be $a \approx 2.37$. In Fig. 5 we show the plot of the non dimensional radius oscillation given by (6.1) and the experimental data.

Then we use the synchronous model (3.5), (3.6) defined in Section 3 to plot the non dimensional pressure close to the inlet $x = 0$. The characteristic values extrapolated from [4] are

$$\dot{R}^*_{ref} = 3.04\ \frac{\mu m}{sec}, \qquad v^*_{ref} = 1.22\ \frac{mm}{sec}, \qquad p^*_{ref} = 0.37\ cmH_2O, \qquad \varepsilon = 2.5 \times 10^{-3}.$$

[4]Recall that δ denotes the oscillation amplitude.

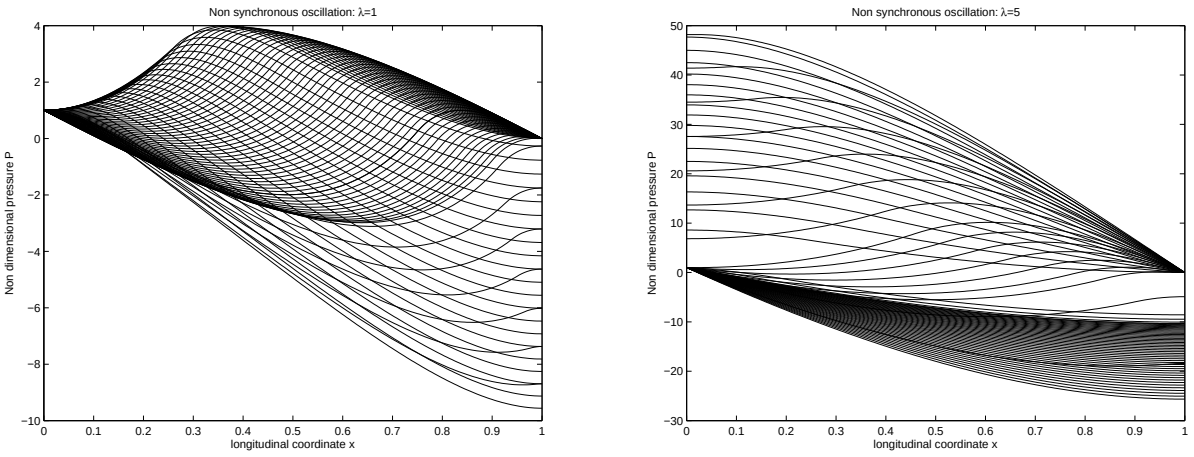

$\lambda = 1$ $\lambda = 5$

Figure 2: Dimensionless pressure profiles $p(x,t)$ for different values of λ, obtained using formulas (4.5)-(4.8).

In Fig. 6 we show the comparison between the experimental data of [4] (Fig. 5, luminal pressure) and the pressure profile predicted by the model. As one can see, the agreement is quite satisfactory, considering the simplicity of the model, which includes just two valves (neglecting their inertia) and operates in a Newtonian context. Numerical simulations of non-synchronous oscillations (peristaltic motion with wavelength comparable to the vessel length, not shown here) did not provide a good fit. Therefore the synchronous two-valve model seems adequate to simulate the phenomenon of vasomotion in the bat wing venules.

7 Conclusions

We have formulated a mathematical model for the phenomenon of vasomotion concerning small vessels (venules), starting from the basic laws of fluid dynamics and exploiting the smallness of the radius/length ratio to derive simpler approximating equations which are nevertheless rather accurate. For simplicity blood has been described as a Newtonian fluid.

Venules provided with valves offer a quite complicated scenario. We have studied the case in which just two valves are present (one at the entrance, one at the exit) in a broader framework, considering both the case of flows driven by travelling contraction/relaxation wave (applicable to larger veins), and the case of synchronous oscillation. The latter can be seen as the limit of the peristaltic motion when the wavelength is much larger than the vessel length. This is not just a mathematical game, since it seems reasonable that an excitation wave propagates along the vessel at a sufficiently high speed to eventually look synchronous. By means of numerical simulations we have shown that the limit of peristalsis driven flow for large wavelength is actually the flow generated by synchronous oscillations, as expected. Moreover, we have compared our simulations with the experimental results of [4] on the vasomotion observed in the bat wing venules, characterized by periodic pressure pulses. We have obtained an agreement which is remarkable, considering the simplicity of the model core. Thus the present model indicates that, at least for the biological case of [4], the scheme with two valves provides a quite reasonable description of the phenomenon. On the contrary, the many valves model discussed in [8] produces a different qualitative behavior which is not compatible with the experimental measures of [4].

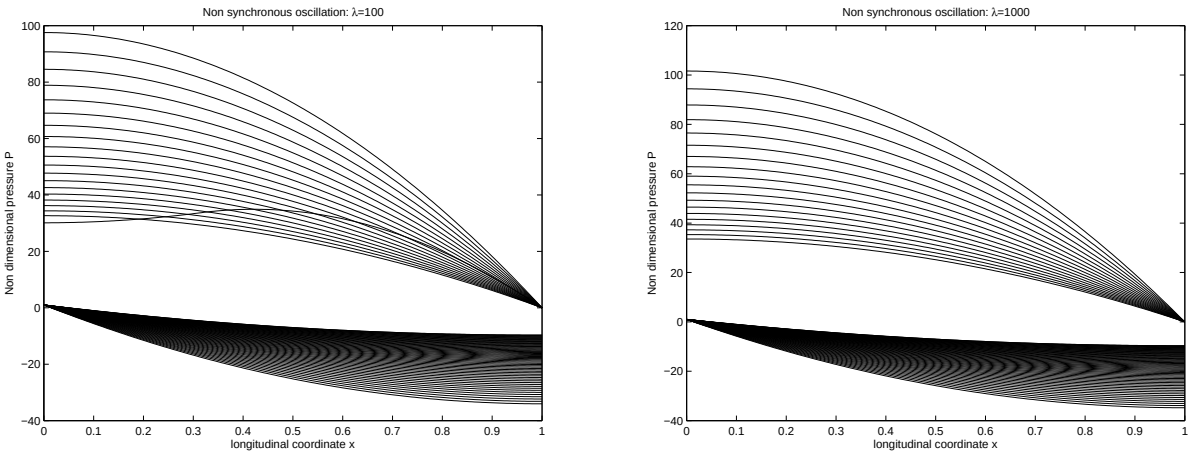

$\lambda = 100$ $\lambda = 1000$

Figure 3: Dimensionless pressure profiles $p(x,t)$ for different values of λ, obtained using formulas (4.5)-(4.8).

References

[1] Aalkjaer C., Nilsson H., Vasomotion: cellular background for the oscillator and for the synchronization of smooth muscle cells, British Journal of Pharmacology, **144** (2005) 605–616.

[2] Brown T. D., Hung T.K., Computational and experimental investigations of two-dimensional nonlinear peristaltic flows, J. Fluid Mech., **83** (1977) 249-272.

[3] de Wit C., Closing the gap at hot spots, Circ Res, **100** (2007) 931-933.

[4] Dongaonkar R. M., Quick C. M., Vo J. C., Meisner J. K., Laine G. A., Davis M. J., Stewart R. H., Blood flow augmentation by intrinsic venular contraction in vivo. Am. J. Physiol. Regul. Integr. Comp. Physiol., **302** (2012) R1436–R1442.

[5] Caggiati A., Phillips M., Lametschwandtner A., Allegra C., Valves in small veins and venules, Eur. J. Vasc. Endovasc. Surg., **32** (2006) 447-452.

[6] Caggiati A., Bertocchi P., Regarding "Fact and fiction surrounding the discovery of the venous valves", Journal of Vascular Surgery, **33** (2001) 1317.

[7] Caggiati A., The venous valves in the lower limbs, Phlebolymphology, **20** (2013) 87-95.

[8] Farina A., Fasano A., Incompressible flows through slender oscillating vessels provided with distributed valves, accepted for pubblication Advances in mathematical sciences and applications (2015).

[9] Franklin K. J., Valves in veins: an historical survey, Proc. Royal Soc. Med. Section of the History of medicine (1927) 1-33.

[10] Fung, Y. C., Yih, C. S., Peristaltic transport, J. Appl. Mech., **35**, 669–675 (1968).

[11] Fusi L., Farina A., Fasano A., Short and long wave peristaltic flow: modeling and mathematical analysis, International Journal of Applied Mechanics, **7** (2015) DOI: 10.1142/S1758825115400141.

[12] Goldschmidtboing F., Doll A., Heinrichs M., Woias P., Schrag H. J., Hopt U. T., A generic analytical model for micro-diaphragm pumps with active valves, J. Micromech. Microeng., **15** (2005) 673–683.

[13] Haddock R.E., Hill C.E., Rhythmicity in arterial smooth muscle, J. Physiol., **56** (2005) 645–656.

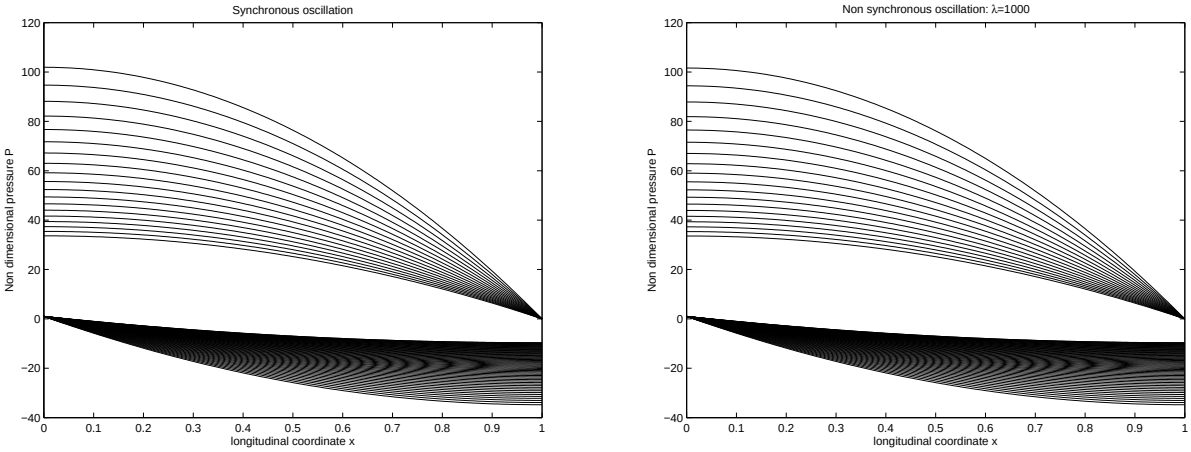

Synchronous oscillation

Non Synchronous oscillation, $\lambda = 1000$

Figure 4: Comparison between the synchronous and non synchronous case for $\lambda = 1000$.

[14] Haddock R. E., Hirst G. D. S., Hill C. E., Voltage independence of vasomotion in isolated irideal arterioles of the rat, Journal of Physiology, **540** (2002) 219–229.

[15] Intaglietta M., Vasomotion and flowmotion: physiological mechanisms and clinical evidence, Vascular Medicine Review, **1** (1990), 1101-112.

[16] Iverson B. D., Garimella S. V., Recent advances in microscale pumping technologies: a review and evaluation, Microfluid Nanofluid, **5**,145–174 (2008) DOI: 10.1007/s10404-008-0266-8.

[17] Jones T. W., Discovery that veins of the bat's wing (which are furnished with valves) are endowed with rhythmical contractility and that the onward flow of blood is accelerated by each contraction, Philos. Trans. R. Soc. Lond., **142** (1852) 131–136.

[18] Kikuchi N., Oden J. T., Contact problem in elasticity: a study of variational inequalities and finite element methods, SIAM Study in Applied Mathematics, Vol. 8, SIAM 1988.

[19] Koenigsberger M., Sauser R., Beny J. L., Meister J. J., Effects of arterial wall stress on vasomotion, Biophysical Journal, **91** (2006) 1663–1674.

[20] Matchkov V. V., Gustafsson H., Rahman A., Boedtkjer D. M., Gorintin S., Hansen A. K., Bouzinova E. V., Praetoriu H. A., Aalkjaer C., Nilsson H., Interaction between Na/K pump and Na/Ca2 exchanger modulates intercellular communication, Circ Res., **100** (2007) 1026 –1035.

[21] Parthimos D., Haddock R. E., Hill C. E., Griffith T. M., Dynamics of a three-variable nonlinear model of vasomotion: Comparison of theory and experiment, Biophysical Journal, **93** (2007) 1534–1556.

[22] Reho J. J., Zheng X., Fisher S. A., Smooth muscle contractile diversity in the control of regional circulations, Am. J. Physiol. Heart Circ. Physiol., **306** (2014) H163–H172.

[23] Rivadulla C., de Labra C., Grieve K. L., Cudeiro J., Vasomotion and neurovascular coupling in the visual thalamus in vivo, PLOS ONE, **6** (2011) 28746.

[24] Shapiro A. H., Jaffrin M. Y., Weinberg S. L., Peristaltic pumping with long wavelengths at low Reynolds number, J. Fluid Mech. **37**, 799–825 (1969).

[25] Singh A. K., Singh D. P., Peristaltic flow of blood through artery with a wave of small amplitude travelling down its wall, International Journal of Mathematics Trends and Technology, **2**, Issue3 (2011).

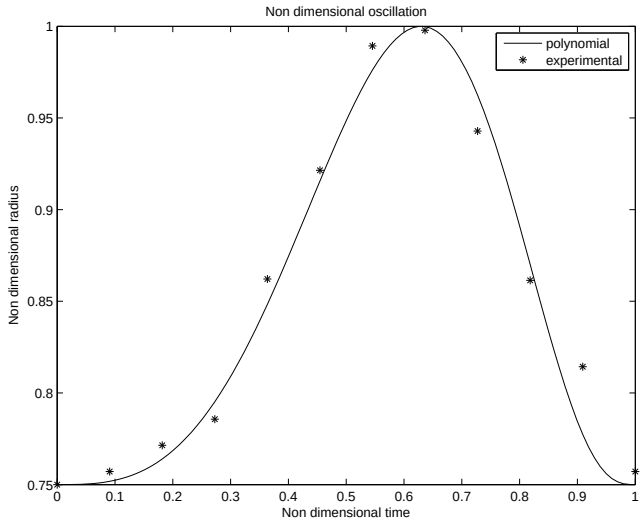

Figure 5: Radius oscillation: comparison with experimental data.

[26] Sisavath S., Jing X., Zimmerman R. W., Creeping flow through a pipe of varying radius, Physics of Fluids, **10**, 2762–2772 (2001).

[27] Takagi D., Balmforth N. J., Peristaltic pumping of viscous fluid in an elastic tube, J. Fluid Mech., **672**, 196–218 (2011).

[28] Uchida S., Aok H., Unsteady flows in a semi-infinite contracting or expanding pipe, J. Fluid Mech., **82**, 371- 387 (1977).

[29] Ursino M., Fabbri G., Belardinelli E., A mathematical analysis of vasomotion in the peripheral vascular bed, Cardioscience, **3** (1992)13-25.

[30] Vajravelu K., Sreenadh S., Devaki P., Prasad K. V., Peristaltic transport of a Herschel–Bulkley fluid in an elastic tube, Heat Transfer - Asian Research, DOI: 10.1002/htj.21137 (2014).

[31] Walker S. W., Shelley M. J., Shape optimization of peristaltic pumping, J. Comput. Phys., **229**, 1260–1291 (2010).

[32] Wang C. Y., Stokes fluid through a tube with bumpy wall, Physics of Fluids, **18**, 078101 (2006).

[33] Xinsheng X., Minzhong W., General complete solutions of the equations of spatial and axisymmetric Stokes flow, Q. Journal Appl. Math, **44**, 537-548 (1991).

[34] Yin F., Fung Y. C., Peristaltic waves in circular cylindrical tubes, J. Appl. Mech., **36**, 579-587 (1969).

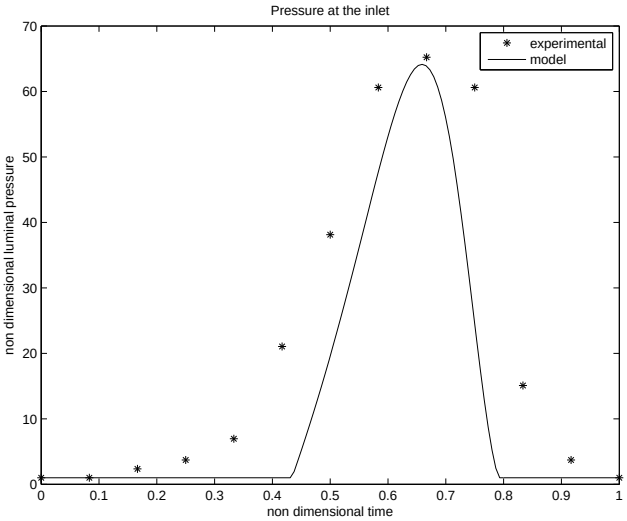

Figure 6: Comparison with experimental data.